This article is published as part of the *Dalton Transactions* themed issue entitled:

New Horizons in Organo-f-element Chemistry

Guest Editor: Geoff Cloke
University of Sussex, UK

Published in issue 29, 2010 of *Dalton Transactions*

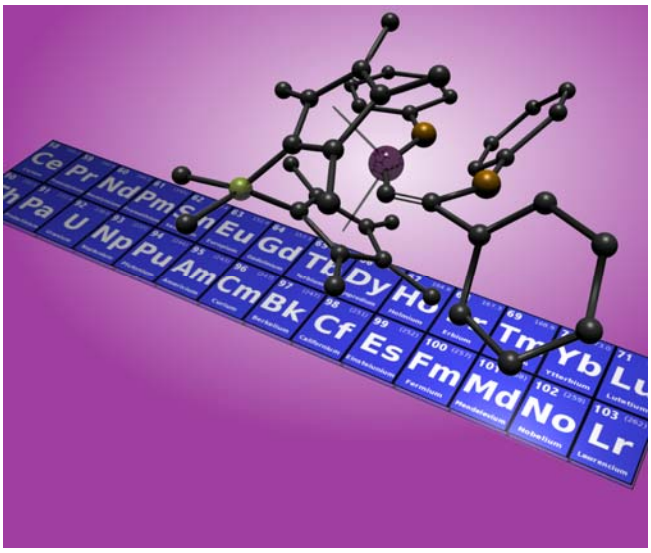

Image reproduced with the permission of Tobin Marks

Articles in the issue include:

PERSPECTIVES:

COMMUNICATIONS:

PAPERS:

Visit the *Dalton Transactions* website for more cutting-edge inorganic and organometallic chemistry research
www.rsc.org/dalton

The reaction of bis(1,2,4-tri-*t*-butylcyclopentadienyl)ceriumbenzyl, Cp'_2CeCH_2Ph, with methylhalides: a metathesis reaction that does not proceed by a metathesis transition state†

Evan L. Werkema,[a] Richard A. Andersen,*[a] Laurent Maron*[b] and Odile Eisenstein*[c]

Received 2nd September 2009, Accepted 1st December 2009
First published as an Advance Article on the web 10th February 2010
DOI: 10.1039/b918103b

The experimental reaction between $[1,2,4\text{-}(Me_3C)_3C_5H_2]_2CeCH_2Ph$ and CH_3X, X = F, Cl, Br, and I, yields the metathetical exchange products, $[1,2,4\text{-}(Me_3C)_3C_5H_2]_2CeX$ and CH_3CH_2Ph. The reaction is complicated by the equilibrium between the benzyl derivative and the metallacycle $[1,2,4\text{-}(Me_3C)_3C_5H_2][(Me_3C)_2C_5H_2C(CH_3)_2CH_2]Ce$, plus toluene since the metallacycle reacts with CH_3X. Labelling studies show that the methyl group of the methylhalide is transferred intact to the benzyl group. The mechanism, as revealed by DFT calculations on $(C_5H_5)_2CeCH_2Ph$ and CH_3F, does not proceed by way of a four-center mechanism, a σ-bond metathesis, but by a lower barrier process involving a haptotropic shift of the Cp_2Ce fragment so that at the transition state the *para*-carbon of the benzene ring is attached to the Cp_2Ce fragment while the CH_2 fragment of the benzyl group attacks CH_3F that is activated by coordination to the metal ion. As a result the mechanism is classified as an associative interchange process.

Introduction

The preparation and reactions of $[1,2,4\text{-}(Me_3C)_3C_5H_2]_2CeH$, abbreviated as Cp'_2CeH, with aliphatic and aromatic hydrofluorocarbons CH_3F and $C_6H_{6-n}F_n$, n = 1–6, respectively, have been published.[1,2,3] These studies were extended to other methylhalides and related compounds, CH_3X, X = Cl, Br, I, OMe, NMe_2 recently.[4] The reactions of these methyl-derivatives with Cp'_2CeH, illustrated by the net reaction in eqn (1), are at first glance a simple metathetical H for X exchange reaction but the reaction mechanism does not proceed by a four-center metathesis transition state.

$$Cp'_2CeH + CH_3X \rightarrow Cp'_2CeX + CH_4 \quad X = F, Cl, Br, I, OMe \quad (1)$$

The combined experimental and computational studies[1,4] showed that the reaction proceeds by a two-step process, the first of which is an intermolecular C–H activation, eqn (2a), that is followed by ejection of CH_2 and trapping by H_2, eqn (2b).

$$Cp'_2CeH + CH_3X \rightarrow Cp'_2CeCH_2X + H_2 \quad (2a)$$

$$Cp'_2CeCH_2X + H_2 \rightarrow Cp'_2CeX + CH_4 \quad (2b)$$

The calculated free energy barriers (called hereafter activation barriers) for the C–H activation step are relatively low, $\Delta G^{\ddagger}$ ranges from 18 kcal mol^{-1} (F) to 14 kcal mol^{-1} (OMe), but the activation barrier for the second step is higher in all cases studied. The calculated activation barrier for a synchronous process that proceeds by way of a metathesis transition state is higher, by about 6 to 8 kcal mol^{-1}, than the second, rate determining step. The physical picture that emerges from the calculations is that the metathesis transition state **A** has negative charge accumulation on H and X and positive charges on Cp_2Ce and on CH_3. It has a higher activation barrier since it resembles $Cp_2Ce^+CH_4X^-$ and CH_4X^- is a high energy species. Accordingly, the reactants choose a two-step pathway in which the transition state for C–H activation, **B**, forms Cp_2CeCH_2X. This is followed by a step in which CH_2 inserts into H_2 with cleavage of the C–X bond forming Cp_2CeX. Experimental evidence for the two-step mechanism was derived by observing that (a) the Me_3C-groups on the Cp′-rings can act as an intramolecular trap for CH_2, when H_2 is absent, as can added cyclohexene, which formed norcarane, and cyclohexane-d_{12} solvent, which formed methylcyclohexane-d_{12}, (b) NMR evidence was obtained for Cp'_2CeCH_2X, X = Cl, Br, I and (c) when X = OMe, $Cp'_2Ce(\eta^2\text{-}CH_2OMe)$ was isolated.[1,4] Thus, the combined computational and experimental studies showed that the two-step pathway proceeding by way of a carbenoid intermediate is general for the CH_3X derivatives studied.

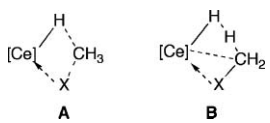

The cerium metallocenes used in these studies, Cp'_2CeCH_2Ph, Cp'_2CeH and Cp'_2CeF are monomeric in the solid state and presumably in solution as well. Hence, they are excellent experimental

[a]*Department of Chemistry and Chemical Sciences Division of Lawrence Berkeley National Laboratory, University of California, Berkeley, California, 94720-1460*
[b]*LPCNO, Université de Toulouse, INSA, UPS, LPCNO, 135 avenue de Rangueil, F- 31077 Toulouse, France, and CNRS, LPCNO, F-31077, Toulouse, France*
[c]*Institut Charles Gerhardt, Université Montpellier 2, CNRS 5253, cc 1501 Place E. Bataillon, F-34095, Montpellier, France*

† Electronic supplementary information (ESI) available: X-ray crystallographic data (CIF), δ *vs.* $1/T$ plots, optimized structures, E and G (in a. u.) for all stationary points. CCDC reference numbers 745664 for $[1,2,4\text{-}(Me_3C)_3C_5H_2]_2CeCH_2Ph$, and 745665 for $[1,2,4\text{-}(Me_3C)_3C_5H_2]_2Ce$(4-methylbenzene). For ESI and crystallographic data in CIF or other electronic format see DOI: 10.1039/b918103b

models for the computational studies, which were carried out using the C_5H_5 metallocenes in the gas phase.

In this article, a combined experimental and computational study of the reaction of Cp'_2CeCH_2Ph, along with its chemical and physical properties, with CH_3X, X = F, Cl, Br, or I, a stoichiometric C–C bond forming reaction, is described, eqn (3).

$$Cp'_2CeCH_2Ph + CH_3X \rightarrow Cp'_2CeX + CH_3CH_2Ph \quad (3)$$

Results

Synthetic studies. Solution and solid state properties of Cp'_2CeCH_2Ph

The synthesis and some physical properties of Cp'_2CeCH_2Ph are reported in an earlier article[2] and additional ones are reported here. Some of the chemical reactions described in this article, along with those reported earlier, are shown in Scheme 1. The benzyl derivative is an excellent precursor to two useful derivatives, the hydride and the metallacycle [1,2,4-$(Me_3C)_3C_5H_2$][$(Me_3C)_2C_5H_2C(CH_3)_2CH_2$]Ce, and their deuterated analogues. Although the benzyl and the 4-methylbenzyl derivatives are isolable, these are the only alkyl derivatives that are thermally stable at room temperature; all attempts to make Me, CH_2CMe_3 or CH_2SiMe_3 derivatives result in alkane elimination and formation of the metallacycle at low temperature.

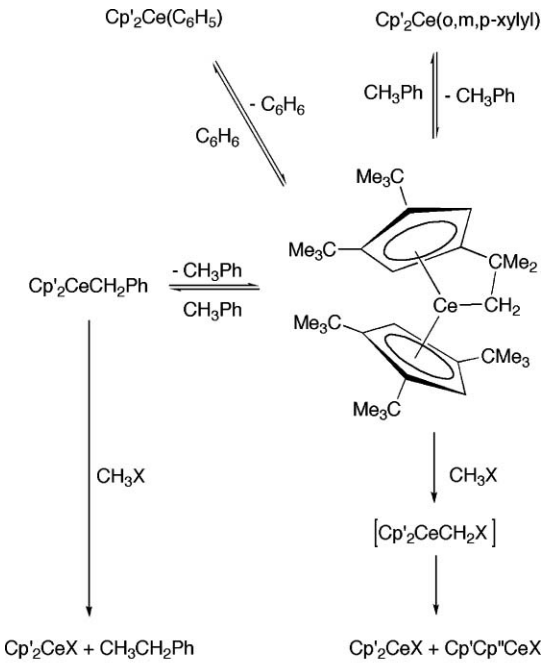

Scheme 1

The ^1H NMR spectrum of the benzyl derivative in C_6D_6 at 19 °C was mentioned previously.[2] The spectrum shows the Me_3C group resonances as three broad singlets in a 1 : 1 : 1 area ratio, inequivalent Cp′-ring CH resonances and one other resonance of area 1 that is assumed to be the *para*-H resonance of the benzyl group; the CH_2 and the benzene ring *ortho* and *meta* resonances are not observed. In order to confirm this assignment, Cp'_2Ce(4-methylbenzyl) is prepared and isolated as outlined in the Experimental section. The variable temperature ^1H NMR spectrum in C_7D_8 of Cp'_2CeCH_2Ph shows that the Me_3C-resonances are in a 2 : 1 area ratio at temperatures greater than 300 K but as the temperature is lowered they decoalesce and reappear as a 1 : 1 : 1 area ratio pattern, see ESI for the δ *vs.* T^{-1} plots for this and the 4-methylbenzyl derivative.† The spectra show that Cp'_2CeCH_2Ph is a fluxional molecule with average C_{2v} symmetry at high temperature but C_s symmetry at lower temperature. In addition, a resonance assigned to the *meta*-H's of the benzyl group is observed at –80 °C as a single resonance in the benzyl and 4-methylbenzyl derivatives, implying that the phenyl ring is either in the plane of symmetry, perpendicular to it, or oscillating about the $CeCH_2$–C(*ipso*) bond generating a time averaged plane of symmetry.

In the solid state, two molecules are found in the asymmetric unit of Cp'_2CeCH_2Ph in equal amounts as shown in Fig. 1. The two molecules in the asymmetric unit, **a** and **b** in Fig. 1 have different orientations of their Cp′ rings and CH_2Ph groups. Since the population of each conformer in the unit cell is equal, their individual free energies are equal, see ESI for crystallographic details.† In conformer **a**, the Cp′ ring carbon atoms are eclipsed, which results in two of the Me_3C groups at the back of the wedge avoiding each other as much as possible resulting in the four Me_3C groups in the front of the wedge being pairwise eclipsed. The Cp′(ring centroid)–Ce(2)–Cp′(ring centroid) angle is 149° and the Ce(2)–C(76)–C(77) angle is 130.4(3)°; the open Ce(2)–C(76)–C(77) angle results in a Ce(2)···C(77) distance greater than 3.7 Å. The other conformer, **b**, is rather different, since the Cp′-ring carbons atoms are staggered with a closed Cp′(ring centroid)–Ce(1)–C′(ring centroid) angle of 138°, 11° less than in **a**. In addition, the Ce(1)–C(35)–C(36) angle of 93.1(4)° is some 37° less than the equivalent angle in **a**, which results in a short Ce(1)–C(36) distance of 3.023(4) Å. The flat phenyl ring is orientated more or less perpendicular to the open wedge of the Cp'_2Ce fragment, and the Ce(1)–C(37) and Ce(1)–C(41) distances are 3.996 and 3.253 Å, respectively, thus, the classification of the benzyl group bonding as η^2 or η^3 is ambiguous; the representation Ce(η^2/η^3–CH_2Ph) seems appropriate.

The solid state molecular structure of Cp'_2Ce(4-methylbenzyl) is shown in Fig. 2. The important distances and angles are given in the caption to Fig. 2. The geometrical parameters for Cp'_2Ce(4-methylbenzyl) are very similar to those of $Cp'_2Ce(\eta^2/\eta^3$-$CH_2Ph)$, Fig. 1b, including the orientation of the cyclopentadienyl rings in the Cp'_2Ce fragment and the orientation of the planar benzene ring.

The geometry of the Ce(η^2/η^3-CH_2Ph) and Ce(η^2/η^3-4-methylbenzyl) fragments, Fig. 1b and 2 respectively, is similar to that found in $(C_5Me_5)_2Ce(\eta^3$-$CH_2Ph)$.[5] In the latter example, the Ce–CH_2–C(*ipso*) angle of 86.0(3)° is even more acute than the equivalent angle in the molecule shown in Fig. 1b, resulting in a Ce···C(*ipso*) and one Ce···C(*ortho*) distance of 2.885(5) Å and 2.882(6) Å, respectively. The Ce–CH_2Ph distance of 2.596(5) Å is identical, to within 3σ, of the equivalent distances in the molecules shown in Fig. 1a, 1b and 2. The benzyl group in the C_5Me_5 derivative has three Ce–C distances less than 3 Å and therefore is classified as a η^3-benzyl. The differing classification clearly is the result of intramolecular steric effects in the metallocene fragments. The solid state crystal structures of metal-benzyl derivatives often

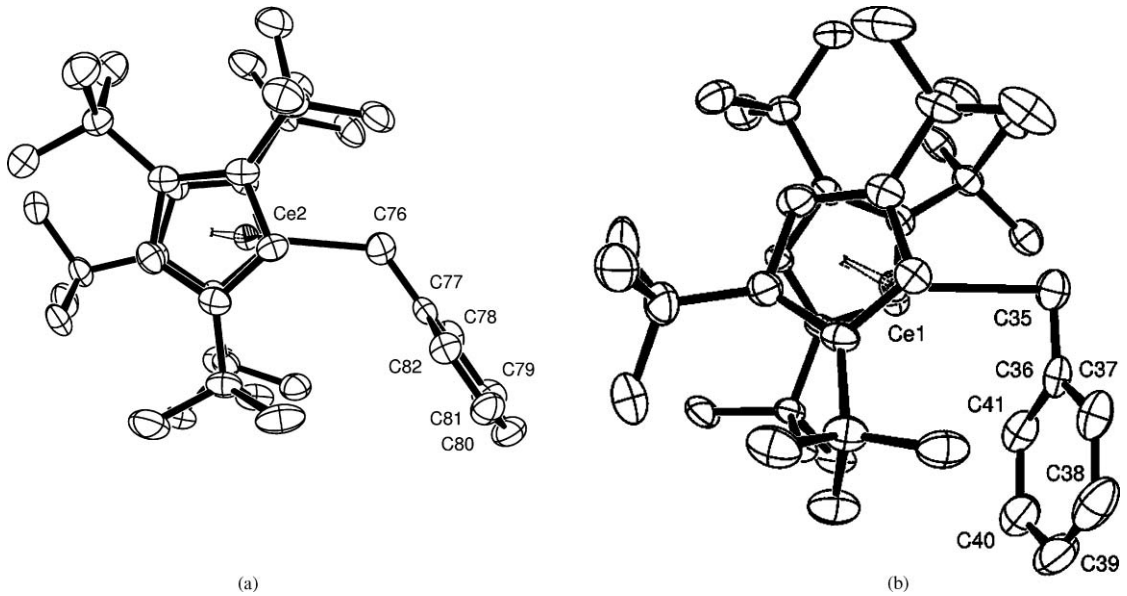

Fig. 1 ORTEP of Cp'_2CeCH_2Ph showing the two molecules in the asymmetric unit, **a**, the conformer with $Ce(\eta^1\text{-}CH_2Ph)$ and, **b**, the conformer with $Ce(\eta^2/\eta^3\text{-}CH_2Ph)$. The non-hydrogen atoms are refined anisotropically and shown as 50% ellipsoids; the hydrogen atoms are not shown, but they are placed in idealized positions and not refined. Selected bond distances (Å) and angles (deg) are **a**: Ce(2)–C(Cp′) = 2.83 ± 0.07 (ave), range 2.752(4)–2.932(4), Ce(2)–Cp′(ring centroid) = 2.54, Cp′(ring centroid)–Ce–Cp′(ring centroid) = 149, Ce(2)–C(76) = 2.577(4), Ce(2)–C(76)–C(77) 130.4(3). **b:** Ce(1)–C(Cp′)= 2.87 ± 0.07(ave), range 2.761(4)–3.010(4), Ce(1)–Cp′(ring centroid) = 2.54, Cp′(ring centroid)–Ce(1)–Cp′(ring centroid) = 138, Ce(1)–C(35) = 2.584(4), Ce(1)–C(36) = 3.023(4), Ce(1)–C(37) = 3.996, Ce(1)–C(41) = 3.253, Ce(1)–C(35)–C(36) = 93.1(4).

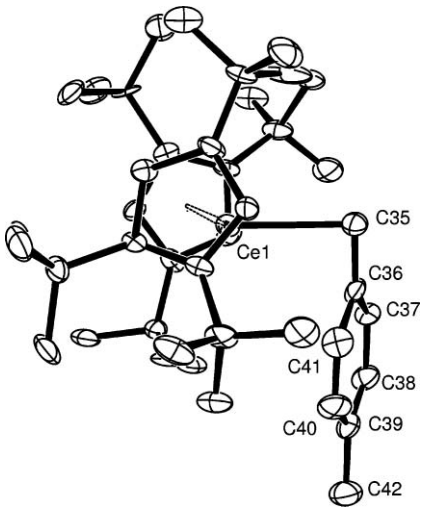

Fig. 2 ORTEP of Cp'_2Ce(4-methylbenzyl), the half molecule of pentane in the asymmetric unit is not shown. The non-hydrogen atoms are refined anisotropically and shown as 50% ellipsoids, the hydrogen atoms are not refined but they are placed in idealized positions and not shown. Selected distances (Å) and angles (deg): Ce–C(Cp′) = 2.86 ± 0.08, range 2.743(8) to 2.995(7), Ce–Cp′(ring centroid) = 2.60, Cp′(ring centroid)–Ce–Cp′(ring centroid) = 138.5, Ce–C(35) = 2.576(7), Ce–C(36) = 2.969(7), Ce–C(37) = 3.933, Ce–C(41) = 3.228, Ce–C(35)–C(36) = 91.7(4°).

have structures in which the M–CH_2–C(*ipso*) angle is much less than 120°, resulting in short M–C(*ipso*) and M–C(*ortho*) distances. This type of structure was first observed in the crystal structure of $Ti(CH_2Ph)_4$,[6,7] $Zr(CH_2Ph)_4$[8] and in f-block benzyl derivatives.[9,10,11]

Solid state behavior of $Cp'_2CeCD_2C_6D_5$

Since the studies described in this article are aimed at understanding the mechanism of the C–C bond formation, eqn (3), it is important to study the deuterated benzyl derivative in order to show whether or not the methyl group of the methylhalide is transferred intact in the ethylbenzene product. The deuterated derivative, $Cp'_2CeCD_2C_6D_5$ is prepared as described in the Experimental section; the d_7-derivative behaves similarly to the d_0-derivative in solution. However, on prolonged storage in the solid state at 20–25 °C in the absence of air and moisture for about three years, the deuteria in the α-CD_2 sites are replaced by hydrogen and one of the Me_3C-groups is enriched with deuteria. The extent of the H/D exchange is determined by solution ^1H and ^2H NMR spectroscopy. Thus, when first prepared and isolated the ^1H NMR spectrum in C_6D_6 consists of three equal area resonances due to the inequivalent Me_3C groups at δ –0.53, –1.80 and –13.19 in addition to the ring methyne resonances. The ^2H NMR spectrum shows only two resonances assigned to deuteria on the *para* and *meta* positions. After standing for about three years, a small portion of the solid was dissolved in C_6D_6 and examined by ^1H NMR spectroscopy. The spectrum is qualitatively the same as that obtained originally, but the ^2H NMR spectrum contains a resonance at δ –13.2 with an area of approximately 2 relative to the *para* and *meta* D-resonances. The resonance at δ –13.2 is identical to one of the cyclopentadienyl ring Me_3C groups mentioned above. Examination of the ^1H NMR spectrum shows that the intensity ratio of the three Me_3C resonances is no longer 9 : 9 : 9 but approximately 9 : 9 : 6.5. In order to confirm the result, the sample was hydrolyzed (H_2O) and the resulting ^1H NMR spectrum shows that the liberated toluene was a mixture of $CH_3C_6D_5$ and $CH_2DC_6D_5$. Hydrolysis (H_2O) of another sample

and examination of the ^{2}H NMR spectrum in C_6D_{12} shows the *ortho*, *meta*, and *para* resonances of toluene in a ratio of 2 : 2 : 1. Since the freshly liberated $(Me_3C)_3C_5H_3$ is a mixture of two isomers that isomerizes to a single isomer on heating,[12] the sample in C_6D_6 was heated at 60 °C for two days. Examination of the ^{1}H NMR spectrum shows the Me_3C resonances in a 9 : 6.5 : 9 area ratio showing that all of the deuteria are on a single Me_3C group. The ^{13}C NMR spectrum shows three Me_3C resonances, only one of which has a shifted 1 : 1 : 1 resonance associated with it, that is clearly due to a Me_2CCH_2D group. Examination of the GC-MS shows the presence of $CH_{3-x}D_xC_6D_5$ isotopologues and Cp′H molecular ion is an envelope that contains the d_0, d_1, d_2 and d_3 isotopologues. Thus, over a prolonged period of time, both deuteria on the α-CD_2 of the benzyl group exchange with one of the CMe_3 groups on the Cp′ ring in the solid state. The solid state behavior of $Cp'_2Ce(CH_2Ph)$ is rather different from that in solution; in solution equilibration occurs between the benzyl derivative and the metallacycle and toluene, Scheme 1. Over reasonably short periods of time in the solid state the equilibration is not observed, but, H/D exchange occurs over long periods of time. The difference is clearly a solid state effect, where the ensemble prevents the equilibrium with metallacycle and toluene and guides the H for D exchange into the unique Me_3C group of the cyclopentadienyl ring; unfortunately, we do not know the molecularity or the mechanism of the exchange. A somewhat related solid state isomerization of $Cp'_2Ce(2,3,4,5\text{-}C_6HF_4)$ was observed earlier.[3]

Solution behavior of Cp'_2CeCH_2Ph

Heating a toluene-h_8 solution of Cp'_2CeCH_2Ph at 60 °C for a day, then storing the sample at 20 °C for an additional day while monitoring the ^{1}H NMR spectrum, shows resonances due to the benzyl derivative and the metallacycle in a ratio of 12 : 1, in addition to four new paramagnetic resonances due, presumably, to the Me_3C groups of at least two $Cp'_2Ce(Ar)$ metallocenes, where Ar represents the isomeric xylyl groups. Hydrolysis (D_2O) and examination of the ^{2}H NMR spectrum shows singlets in the aromatic region and a triplet (J_{HD} = 2.1 Hz) in the methyl region in an area ratio of 2.5 : 1 : 1 : 6. This result is consistent with the presence of the four possible toluene-d_1 isotopomers in which deuteria are in the four possible sites, implying that all possible xylyl metallocenes as well as the benzyl metallocene are formed in toluene solvent. The 4-methylbenzyl complex, though stable in the solid state, is also in equilibrium with the metallacycle and *p*-xylene analogous to that of the benzyl complex.

This deduction is strengthened by allowing the deuterated metallacycle-d_{53} to react with an excess of C_7D_8 in an NMR tube for one day at 60 °C and an additional day at 20 °C. After removing the C_7D_8 and redissolving the residue in C_6D_{12}, the ^{2}H NMR spectrum shows resonances due to $(Cp'\text{-}d_{27})_2CeCD_2C_6D_5$ and four additional resonances at the same chemical shift and with comparable intensities as above. Upon hydrolysis (H_2O), the ^{1}H NMR spectrum in C_6D_{12} shows two new aromatic and one aliphatic resonances of toluene. These results strengthen the deduction reached above, *viz.* the metallacycle reacts with the aromatic and aliphatic C–H bonds of toluene; a similar H for D exchange was shown earlier for methane.[1] Accordingly, solvents for reactions of the benzyl derivative must be chosen carefully in order to minimize complications due to H/D exchange reactions. Thus in pentane or in cyclohexane, the metallacycle is isolated or generated in pure form. In benzene, the phenyl derivative may be isolated or generated in pure form.[2] Although the equilibrium between the benzyl and the metallacycle is, on one hand, useful as it allows access to labeled cyclopentadienyl compounds, on the other hand, it complicates the reactions studied in this article, since the metallacycle reacts with the methylhalides[4] and deuterium labeling is essential to unravel these pathways.

Reactions of Cp'_2CeCH_2Ph with CH_3X, X = F, Cl, Br, I

Addition of CH_3F to a solution of Cp'_2CeCH_2Ph in C_6D_6 at 20 °C in an NMR tube results in a decrease in the resonances due to the benzyl and the appearance of the resonances due to Cp'_2CeF. After one day the ratio of Cp'_2CeCH_2Ph to Cp'_2CeF is about 2 : 1 and after two days, the resonances due to Cp'_2CeCH_2Ph are absent and those due to Cp'_2CeF and $Cp'Cp''CeF$ [Cp″ = $(Me_3C)_2(EtMe_2C)C_5H_2$] are present in comparable amounts. The appearance of Cp′Cp″CeF is a clear indication that Cp'_2CeCH_2F forms, as illustrated in Scheme 1.[1,4] The ^{1}H NMR spectrum also contains resonances due to CH_3CH_2Ph and CH_3Ph in an approximate area ratio of 1 : 4 and the total amount of these two aromatic hydrocarbons corresponds to that expected from the amount of Cp'_2CeCH_2Ph originally present. Qualitatively, the ratio of CH_3CH_2Ph to CH_3Ph (1 : 4) shows that the reaction of Cp'_2CeCH_2Ph with CH_3F is slower than the benzyl to metallacycle and toluene equilibrium.

In order to be sure that ethylbenzene is formed from Cp'_2CeCH_2Ph, the reaction of $Cp'_2Ce(CD_2C_6D_5)$ and CH_3F in C_6D_6 was followed by NMR spectroscopy. After two days at 20 °C, all of the resonances due to $Cp'_2Ce(CD_2C_6D_5)$ have disappeared and the only resonances observed in the ^{2}H NMR spectrum are due to $CH_3CD_2C_6D_5$ and $CHD_2C_6D_5$. Hydrolysis (H_2O) and analysis of the hydrolysates by GC-MS shows the presence of Cp′H, Cp″H, $CHD_2C_6D_5$ and $CH_3CD_2C_6D_5$. These results clearly show that the methyl group in CH_3F is transferred intact to the benzyl group and that the toluene is derived from the equilibrium reaction of the benzyl and the metallacycle.

The reaction of Cp'_2CeCH_2Ph with MeX, X = Cl, Br and I in C_6D_{12} proceeds in a manner similar to that of CH_3F, except that resonances due to Cp'_2CeCH_2X appear and disappear over time. As shown previously, the formation of Cp'_2CeCH_2X is due to reaction of the metallacycle with CH_3X, which reacts further forming Cp'_2CeX and Cp′Cp″CeX.[4] In addition, CH_3CH_2Ph is observed in each case. In order to show that the ethylbenzene is formed by direct reaction of Cp'_2CeCH_2Ph with CH_3X, rather than insertion of CH_2 from Cp'_2CeCH_2X into toluene formed along with the metallacycle, the reactions with CD_3Br and CD_3I were studied. Addition of either CD_3Br or CD_3I to Cp'_2CeCH_2Ph in an NMR tube in C_6D_{12} proceeds similar to that of CH_3Br or CH_3I. After hydrolysis (H_2O), analysis by GC-MS shows the presence of Cp′H, Cp″H-d_2, CH_3Ph-d_0 and CH_3CH_2Ph-d_3. The ^{2}H NMR spectrum of the solution, before hydrolysis, shows that all of the deuteria in the ethylbenzene are on the terminal carbon, CD_3CH_2Ph, and no CHD_2CH_2Ph or CHD_2CHDPh are detected. Repeating the reaction between Cp'_2CeCH_2Ph and CD_3Br in C_6H_6 solvent and monitoring the reaction by ^{2}H NMR spectroscopy shows only resonances due to CD_3CH_2Ph. Thus, the methyl group

of either CD_3Br or CD_3I are transferred intact and the toluene, formed from the equilibrium between the benzyl derivative and the metallacycle, does not trap the CD_2 fragment nor does the benzyl group accept a deuteron from CD_3X to form CH_2DPh that traps the CD_2 fragment, Scheme 1.

The reaction of Cp'_2Ce(4-methylbenzyl) with CH_3F in C_6D_{12} is similar to that of the benzyl, *viz.*, Cp'_2CeF and $Cp'Cp''CeF$ are formed along with *p*-xylene and 4-ethyltoluene; the latter two products are formed from the equilibrium between the 4-methylbenzyl derivative and the metallacycle, and direct reaction with CH_3F, respectively. The reactions of Cp'_2Ce(4-methylbenzyl) with CH_3X, X = Cl, Br, and I, proceed with similar rates and products as with Cp'_2CH_2Ph.

Reactions of Cp'_2CePh with CH_3F

During the studies described above, some of the reactions of Cp'_2CeCH_2Ph with methylhalides are studied in C_6D_6 or C_6H_6 solvents rather than in C_6D_{12}. A potential complication of reactions in C_6H_6 is exchange that results in the formation of Cp'_2CePh and toluene, as noted previously.[2] If the phenyl derivative reacts with CH_3X then another route for formation of toluene is available. In order to examine this possibility, Cp'_2CePh and $Cp'_2Ce(C_6D_5)$ were prepared and allowed to react with CH_3F. When Cp'_2CePh and CH_3F are mixed in an NMR tube in C_6H_6, resonances due to Cp'_2CeF and $Cp'Cp''CeF$ appear within an hour. After two days at 20 °C, the ratio of Cp'_2CePh to the fluorides (Cp'_2CeF and $Cp'Cp''CeF$) is 6 : 5 and after five days the ratio is 1 : 4. Hydrolysis (H_2O) and analysis by GC-MS shows the presence of toluene as well as Cp′H and Cp″H. Repeating the reaction of CH_3F with $Cp'_2Ce(C_6D_5)$ in C_6D_6 shows that the toluene formed is $CH_3C_6D_5$ by ^2H NMR spectroscopy and examination of the hydrolysate (H_2O) by GC-MS after the resonances due to $Cp'_2Ce(C_6D_5)$ have disappeared (42 days). Thus, the reaction of Cp'_2CePh with CH_3F to give CH_3Ph is much slower than that of Cp'_2CeCH_2Ph. In addition these two experiments show that benzene does not trap the CH_2-fragment resulting from Cp'_2CeCH_2F.

Computational studies

Model

The mechanism for the reaction of Cp'_2CeCH_2Ph and CH_3F was analyzed by DFT(B3PW91) calculations with the methodology used in all our previous studies on the reactivity of lanthanide complexes with a variety of small molecules, including CH_3X.[1,2,4,13] Cp'_2CeCH_2Ph is modeled by Cp_2CeCH_2Ph, which decreases significantly the steric effects of the metallocene fragment. This model was appropriate in the study of the reaction of CH_3X (X = F, Cl, Br, I, OMe, NMe_2) with Cp'_2CeH.

Structure of $Cp_2Ce(CH_2Ph)$

The calculated structure of the benzyl complex shown in Fig. 3 is in good agreement with the structure shown in Fig. 1b, one of the two molecules found in the crystal structure of Cp'_2CeCH_2Ph and in Fig. 2, the 4-methylbenzyl structure. The C(1)–C(2) distance of 1.44 Å, is between that expected for a single and a double bond. The cerium is bonded to the benzyl group by way of C(1) at a distance of 2.64 Å but the cerium atom is also close to C(2) (2.78 Å)

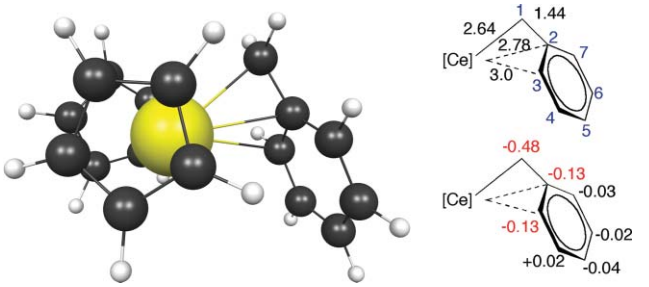

Fig. 3 The optimized DFT (B3PW91) structure of $Cp_2Ce(\eta^3\text{-}CH_2Ph)$ with, top, distances in Å, and, bottom, NBO charges in the CH or CH_2 groups of the benzyl. [Ce] represents Cp_2Ce. The red color indicates the most negatively charged atoms in the benzyl group. Numbering of carbon atoms in the benzyl group is in blue.

and the two *ortho* carbon atoms, C(3) and C(7), of the phenyl ring (3.0 and 3.4 Å). This leads to an acute Ce–C(1)–C(2) angle of 80°, which compares reasonably well with the experimental angle of 92–93°. As a consequence of the more acute Ce–C(1)–C(2) angle in the calculated structure, the distances between Ce and the *ortho* carbons are significantly shorter than in the crystal structures. The modeling of the Cp′ ligand by the less bulky Cp ligand is most likely the origin of the smaller Ce–C(1)–C(2) angle in the calculated structure. The benzyl group is not an η^1-benzyl since the benzene ring is orientated with its flat, open-face towards the open wedge of the Cp_2Ce fragment. This orientation is the result of the acute Ce–C(1)–C(2) angle and the negative charge density distribution around the benzene ring. Since this stereochemistry is observed in one of the two molecules in the crystal structure of Cp'_2Ce(benzyl) and in Cp'_2Ce(4-methylbenzyl), this orientation is not due to steric effects. The calculated structure of Cp_2Ce(4-methylbenzyl), is similar to that of the benzyl, including the acute Ce–C(1)–C(2) angle of 80°. The other molecule in the solid state crystal structure of Cp'_2Ce(benzyl) shows an η^1-benzyl group with a Ce–C(1)–C(2) angle of 130°. No calculated structure with a large Ce–C(1)–C(2) angle is located as a minimum on the potential energy surface, an additional indication that the η^3-benzyl is an energy minimum.

The calculated structure, with a Ce–C(1)–C(2) angle of 80°, can be understood by considering how the Cp_2Ce^+ fragment interacts with a benzyl anion. In an isolated benzyl anion, the π density is mostly on C(1), the *ortho* C(3) and C(7) and the *para* carbon C(5). Interaction between the Cp_2Ce^+ fragment and the benzyl ligand polarizes the π electron density. In the optimal structure, the electron π density of the benzyl ligand is mainly localized on C(1), C(2) and an *ortho* carbon C(3) with only a small amount localized on the other *ortho* carbon C(7), the *meta* and *para* carbons C(4, 5 and 6). According to the NBO analysis, the charge (sum of the charges on carbon and adjacent hydrogens) on C(1) is –0.48 and on each *ipso* C(2) and *ortho* C(3) it is –0.13. The other carbon atoms have charges smaller than ± 0.04. Therefore the bonding between the Cp_2Ce fragment and the benzyl group becomes allylic in character and the most stable structure has an η^3-benzyl as is found in $(C_5Me_5)_2Ce(\eta^3\text{-}CH_2Ph)$.[5]

Finally the good agreement between the calculated structure and one of the two molecules in the crystal structures validates the choice of Cp_2CeCH_2Ph as a model for Cp'_2CeCH_2Ph.

Pathways for the reaction of Cp_2CeCH_2Ph with CH_3F

The σ-bond metathesis pathway is considered first. In this one-step concerted reaction, the transition state has the usual kite-shaped structure. The CH_2 group of the benzyl and F of CH_3F occupy the α-positions of the four-membered ring and the CH_3 group occupies the β-site. The four-membered ring has angles which are close to 90° and a long C ··· C distance. The Gibbs free energy of this transition state is 50.6 kcal mol^{-1}, a barrier that is significantly higher than the 31.1 kcal mol^{-1} free energy barrier for the metathesis transition state in the H for F exchange in the reaction of Cp_2Ce–H and CH_3–F. The structure of the metathesis transition state is shown in Fig. 4. The high activation barrier makes a σ-bond mechanism improbable.

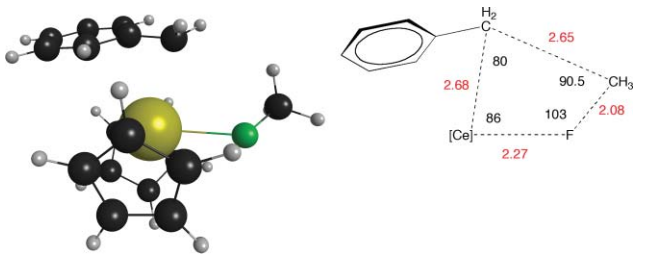

Fig. 4 Transition state for σ-bond metathesis for the reaction between Cp_2CeCH_2Ph and CH_3F, distances in Å, angles in degrees.

The two-step pathway, which begins by a proton transfer from the methyl group of CH_3F to the benzyl ligand, is the next alternative considered. The starting structure for the proton transfer step is the adduct between Cp_2CeCH_2Ph and CH_3F; the interaction is rather weak and the binding energy of 5.6 kcal mol^{-1} does not compensate fully the loss of entropy, which leads to an adduct 4.8 kcal mol^{-1} above the separated Cp_2CeCH_2Ph and CH_3F reactants. This adduct is not shown in Fig. 7. The free energy of the proton transfer transition state is 32.4 kcal mol^{-1}, which is again significantly higher than the value of 18 kcal mol^{-1} found for Cp_2CeH and CH_3F and higher than the value of 21.6 kcal mol^{-1} calculated for the proton transfer in the reaction of Cp_2CeCH_3 and CH_3F (Fig. 5). The proton transfer leads to toluene and Cp_2CeCH_2F, which is 4.1 kcal mol^{-1} higher in energy than Cp_2CeCH_2Ph and CH_3F. The transition state for the following step, insertion of CH_2 into an aliphatic C–H bond of toluene forming ethylbenzene and Cp_2CeF, has a free energy barrier of 36.2 kcal mol^{-1}. While the activation energy barriers for this two-step process are not low, they are significantly lower than that of the σ-bond metathesis. However, the methyl group is not transferred intact in this process, which disagrees with the experimental result and another physical process needs to be discovered.

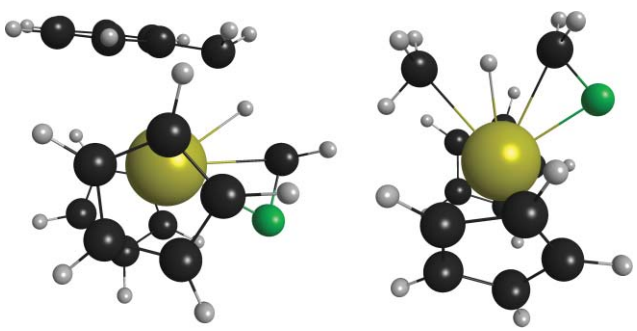

Fig. 5 Transition states for proton transfer for the reaction of, left, Cp_2CeCH_2Ph and CH_3F and, right, Cp_2CeCH_3 and CH_3F.

A transition state that connects directly Cp_2CeCH_2Ph and CH_3F forming Cp_2CeF and ethylbenzene and agrees with the labeling experiment has a Gibbs free energy barrier of 33.3 kcal mol^{-1}. In this transition state, the Cp_2Ce fragment is 2.95 Å from C(5), the *para* carbon of the benzyl group and 3.15 Å from the two *meta* carbons C(4) and C(6), and 4.55 Å from the methylene carbon, C(1) (Fig. 6). Thus, the Cp_2Ce fragment is not bonded to the CH_2 group of the benzyl fragment but is attached by way of C(5). The C(1)–C(2) distance of 1.39 Å is shorter than in the benzyl complex where it is 1.44 Å (Fig. 3). The CH_3F molecule is bonded to Ce by way of F, and the CH_3 group is 2.47 Å from the unbound CH_2 group of the benzyl fragment with an $C(CH_2)$–$C(CH_3)$–F angle of 160°. Thus the CH_2 group is ideally orientated for a nucleophilic attack on the CH_3 group of CH_3F whose electrophilicity is increased by the coordination of F to the positively charged Cp_2Ce fragment, an associative interchange, I_A, mechanism.[14] This transition state forms the C–C bond and cleaves the C–F bond without rearranging the hydrogen atoms and therefore the CH_3 group of CH_3F is transferred intact to form the ethylbenzene in accord with experiment.

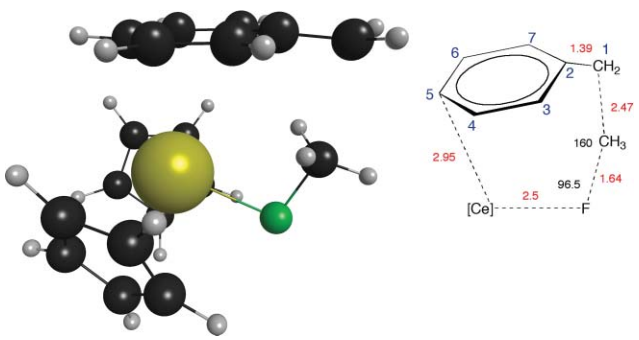

Fig. 6 The transition state in the reaction of Cp_2CeCH_2Ph and CH_3F, distances in Å and angles in degrees.

This pathway is also examined for the 4-methylbenzyl complex. Remarkably the free energy barrier is 34.3 kcal mol^{-1}, only 1 kcal mol^{-1} higher than that calculated for the benzyl complex.

Discussion

Comparison of the free energy profiles of the three pathways allows us to eliminate the σ-bond metathesis as a pathway for the formation of ethylbenzene since the free energy barrier is significantly higher than the other two calculated pathways (Fig. 7). The present result generalizes the results found for the H for X exchange reactions between Cp_2CeH and CH_3X, for which the σ-bond metathesis pathway is also energetically unfavorable, that is, the kite-shaped transition state is a high energy process when a methyl group is in the β-position, regardless of the nature of the chemical groups at the α-positions.

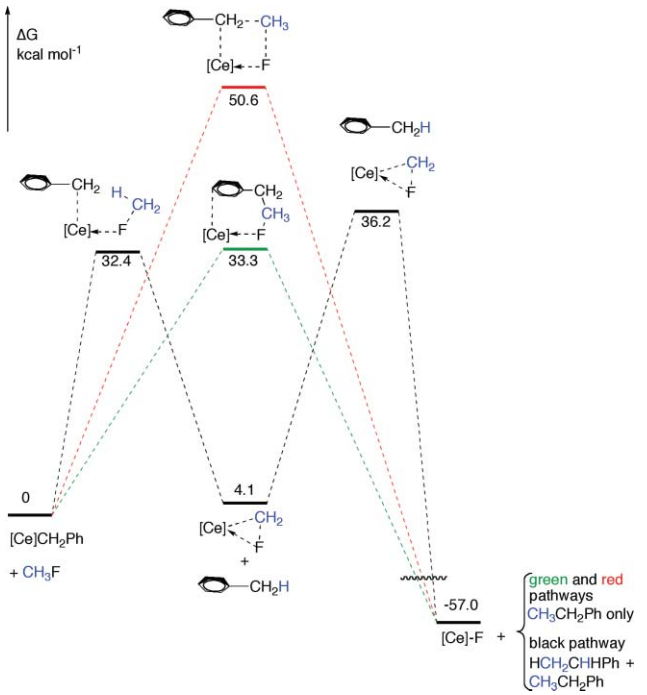

Fig. 7 Free energy profiles in kcal mol^{-1} for the reaction of Cp_2CeCH_2Ph and CH_3F. [Ce] represents the Cp_2Ce fragment. The I_A process is in green, the two-step process (proton transfer, CH_2 insertion) is in black and the σ-bond metathesis is in red.

The free energy barrier of the proton transfer step in the reaction of Cp_2CeR with CH_3F increases from 18 kcal mol^{-1} to 22 and to 32 kcal mol^{-1} when R is H, CH_3 and benzyl, respectively. The proton transfer has the lowest energy barrier when R is H, since this ligand concentrates a large negative charge in a spherical orbital. In the methyl complex, the negative charge is localized in a hybrid orbital carrying the density on the negatively charged methyl group, *i.e.* the overlap with the proton is less. As the bond between the methyl group and the incoming proton develops, the Ce–Me bond distorts significantly as the methyl group tilts in order to share its electron density with the proton (Fig. 5). In the case of benzyl, two factors contribute to the increase in the free energy barrier for proton transfer; (i) the negative charge of the benzyl is dispersed over the whole group and its CH_2 group forms a weaker C···H interaction (this is also shown by the difference between the deprotonation enthalpies of CH_4 and toluene, which are 417 and 374 kcal mol^{-1}, respectively[15]) and (ii), the distortion that occurs in the methyl group cannot be as strong in the benzyl group since the distortion will force the benzene ring and the Cp_2Ce fragment into close contact. As a result, the energy barrier for the proton transfer step between Cp_2CeCH_2Ph and CH_3F is higher than in Cp_2CeMe.

The calculated free energy barriers for the I_A mechanism and the proton transfer pathways are similar (Fig. 7). The relative energy of these transition states are influenced presumably by the presence of the six bulky Me_3C groups on the two cyclopentadienyl ligands in the experimental systems. The Me_3C groups not only create steric effects in the ground and transition states but they modify the angle between the two cyclopentadienyl rings that influences the interaction between the metal with the other ligands. The computational model does not indicate a preference for either pathway but the experiments show that the methyl group is transferred intact, which is only consistent with the I_A mechanism.

Experimentally, the reactions between Cp'_2CeCH_2Ph and CH_3X are complicated by the equilibrium between the benzyl derivative and the metallacycle and toluene, since the metallacycle also reacts with CH_3X, Scheme 1. The relative rates of reaction of the benzyl with CH_3X *versus* the formation of metallacycle and toluene can be estimated by the relative amount of CH_3CH_2Ph and CH_3Ph formed. This is reliable, however, only when X = F, since the reaction of this halide is clean and relatively rapid with the benzyl and metallacycle. At 20 °C, the ratio of CH_3CH_2Ph to CH_3Ph is 1 : 4, showing that the C–C bond forming reaction is slower than the elimination of toluene. The ratio of CH_3CH_2Ph to *p*-xylene in the reaction of Cp'_2Ce(4-methylbenzyl) with CH_3F is similar, implying no appreciable substituent effect on the rate of reaction, consistent with the calculations. However, the rate of reaction of the benzyl derivative is much faster than that of the phenyl, presumably because a benzyl group is a better nucleophile than a phenyl group. The experimental studies give only qualitative mechanistic information about the C–C bond forming reaction, however, the computational studies show that the benzyl group is indeed behaving as a nucleophile in the transition state for the $PhCH_2$ for F group exchange reaction. In the transition state, the benzyl group is attached at only one point, the *para* carbon of the benzene ring. An NBO analysis of the individual atoms in the benzyl group in the ground state and the transition state shows that: (i) the variation in the charges at the *ipso*, *ortho* and *meta* carbon are small, (ii) the negative charge on the *para*-carbon increases by almost 0.2 e and (iii) the negative charge on the methylene carbon decreases by 0.30 e (Fig. 8). The charge redistribution can be understood by considering three of the valence bond structures that represent the benzyl anion (Fig. 8, bottom). Their relative weights are determined by the position of the Cp_2Ce fragment. In the ground state, resonance structures A and B dominate while in the transition state, resonance structures A and C dominate. Thus, from the ground to the transition state, the haptotropic shift of the Cp_2Ce fragment is energetically facilitated by the continuous interaction with the electron density on the benzyl anion as it moves to the *para*-carbon. It should be noted that the net charge on the benzyl anion is almost constant during this haptotropic shift; what changes is the localization of the sites of the density. As mentioned earlier, it is the large positive charge on the Cp_2Ce fragment that controls and guides the charge redistribution as the molecules reach the transition state in the exoergic reaction.

Several X-ray crystal structures of metal-benzyl compounds are informative models for the transition state of the Cp'_2CeCH_2Ph and CH_3F reaction. The solid state structure of the ion-pair, $[(C_5Me_5)Zr(CH_2Ph)_2]^+[PhCH_2B(C_6F_5)_3]^-$, shows that the two benzyl groups in the cation are bonded to zirconium in an η^3- and η^7-fashion; in connection to the present article, the geometry of the η^7-bonded benzyl group is of particular interest, since the *ortho*- and *meta*-carbons are coplanar while the *para*- and *ipso*-carbons are out of the plane by 13° and 15°, respectively, and the CH_2 fragment is out of the plane defined by the *ortho*- and *ipso*-carbons by 21°. Thus, the benzene ring is in a "boat conformation" and the C–C distances are consistent with the dominant influence of resonance structure C.[16] Two recent solid state crystal structures

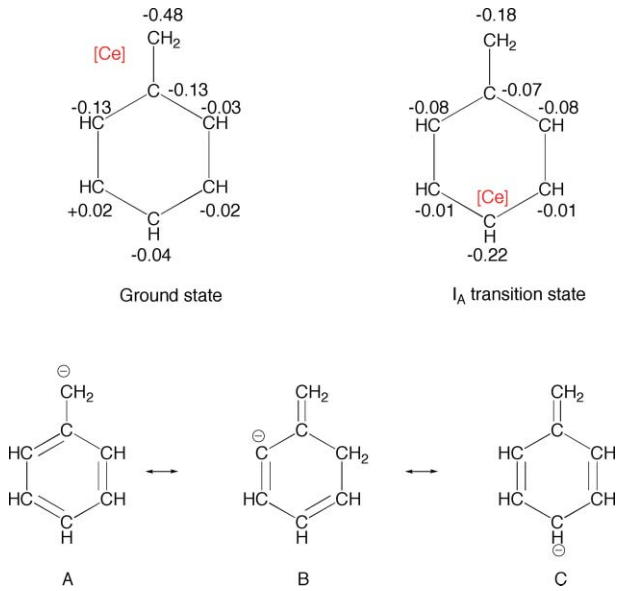

Fig. 8 NBO charges on the benzyl ring in, left, Cp_2CeCH_2Ph and right, the I_A transition state. The position of the Cp_2Ce fragment is qualitatively reproduced by its projection on the benzyl plane and is indicated by [Ce].

of thorium complexes with benzyl groups are noteworthy, since the benzyl group in the anion in both of them, $PhCH_2B(C_6F_5)_3^-$, is attached to a Th^{IV} cation in an η^6-fashion. In both anions, the CH_2 fragment bonded to the $B(C_6F_5)_3$ group is out of the plane of the benzene ring by 10–12° and the Th–C distances to the benzene ring vary in the order C(*para*) < C(*meta*) < C(*ortho*) ≪ C(*ipso*).[17,18]

The possibility of multihapto interactions between a positive ion, Li^+, Na^+, K^+, Rb^+, Cs^+, and a benzyl anion has been shown with MP2 calculations.[19] The size of the metal ion is important since there is a preference for η^3-benzyl for Li and Na and η^7-benzyl for the larger ions. In addition, calculations show that in the case of Li^+, a haptotropic shift from η^3 to η^5-benzyl occurs with a very low energy barrier. The crystal structures and calculated ground state structures show that the interaction between a benzyl anion and a positively charged metal fragment ranges from η^1 to η^7. In these structures the CH_2 group is close to the metal ion fragment and the classification of the bond type is determined by the distance between the metal ion and the carbon atoms of the arene. The calculated transition state for the carbon–carbon bond forming reaction shows that the CH_2 group is not attached to the metal and therefore the electron density is available for a nucleophilic attack on the methyl group of CH_3F, whose electrophilicity is enhanced by the coordination of the fluorine atom to Cp_2Ce.

Conclusion

The net reaction between Cp'_2CeCH_2Ph and CH_3X (X = F, Cl, Br, I) yields Cp'_2CeX and CH_3CH_2Ph. Calculations carried out for X = F show that the mechanism of the benzyl for fluoride exchange reaction does not proceed by way of a simple four-center transition state, since a lower barrier process in which the benzyl group is attached at the *para* position to the Cp_2Ce fragment leaves the CH_2 group free to act as a nucleophile forming the C–C bond with CH_3F. This yields ethylbenzene or, when $Cp'_2CeCD_2C_6D_5$ is used in the experimental studies, $CH_3CD_2C_6D_5$ without scrambling the hydrogens of the CH_3 group. In this mechanism, the metal allows the CH_2 fragment of the benzyl group to behave as a nucleophile towards the CH_3F molecule, which is itself activated by the metal to behave as an electrophile.

Experimental details

General

All manipulations were performed under an inert atmosphere using standard Schlenk and dry box techniques. All solvents were dried and distilled from sodium or sodium benzophenone ketyl. Anhydrous methyl fluoride, methyl chloride, and methyl bromide were used without further purification. Methyl iodide was obtained commercially and purified by distillation onto activated 4 Å molecular sieves. NMR spectra were recorded on Bruker AV-300 or AV-400 spectrometers at 20 °C in the solvent specified. J-Young NMR tubes were used for all NMR tube experiments. Electron impact mass spectrometry and elemental analyses were performed by the microanalytical facility at the University of California, Berkeley. The abbreviation Cp′ is used for the 1,2,4-tri-*tert*-butylcyclopentadienyl ligand. Unless otherwise specified, samples for GC-MS were prepared by adding a drop of nitrogen-purged H_2O, agitating, and allowing the samples to stand closed for 10 min. The samples were then dried over magnesium sulfate, filtered, and diluted ten-fold with pentane. A 1 μL sample was injected into a HP6890 GC system with a J&W DB-XLB universal non-polar column, attached to an HP5973 Mass Selective Detector.

$Cp'_2CeCD_2C_6D_5$. $C_6D_5CD_2MgCl$ was prepared by slowly adding a solution of benzyl chloride-d_7 (1 g, 7.5 mmol) in 10 mL of diethyl ether to magnesium turnings (0.18 g, 7.4 mmol) in 10 mL of diethyl ether and heating the resulting pale blue solution at reflux for 1 h. The solution was filtered and titrated with a standard 0.1 N aqueous HCl solution; the concentration of $C_6D_5CD_2MgCl$ was determined to be 0.25 M. $Cp'_2CeOTf{\cdot}0.5$ hexane[2] (3.44 g, 4.3 mmol) was dissolved in 30 mL of diethyl ether and $C_6D_5CD_2MgCl$ solution (17 mL, 0.25 M in diethyl ether, 4.25 mmol) was added *via* syringe. The solution immediately changed from yellow to red, and became cloudy within 5 min. After 5 min the solvent was removed under reduced pressure, yielding a red powder. The ^1H NMR spectrum of the crude product contained resonances corresponding to Cp'_2CeCl[20] and CMe_3 resonances identical to those of $Cp'_2CeCH_2C_6H_5$;[2] the two species were present in approximately a 1 : 1 ratio. The red solid was extracted with 25 mL of pentane to isolate $Cp'_2CeCD_2C_6D_5$, and the yellow solid residue was extracted further with 25 mL of toluene to recover the remaining Cp'_2CeCl. The volume of the pentane solution was reduced to 10 mL and cooled to −10 °C, giving red blocks. Yield, 0.78 g (1.1 mmol, 26%). The ^1H NMR spectrum contained resonances identical to the CMe_3 and ring C–H resonances observed in $Cp'_2CeCH_2C_6H_5$, ^1H NMR (C_6D_6): δ 50.63 (2H, $\nu_{1/2}$ = 245 Hz), 13.25 (2H, $\nu_{1/2}$ = 245 Hz), −0.53 (18H, $\nu_{1/2}$ = 190 Hz), −1.80 (18H, $\nu_{1/2}$ = 195 Hz), −13.19 (18H, $\nu_{1/2}$ = 45 Hz). The resonance at 50.63 ppm was incorrectly reported as a fold-over resonance at −32.62 ppm in a previous publication.[2] The ^2H NMR spectrum contained resonances consistent with the aromatic benzyl group resonances observed in the ^1H NMR

spectrum of $Cp'_2CeCH_2C_6H_5$,[2] ^2H NMR (C_6D_6): δ 4.18 (2H, $\nu_{1/2}$ = 50 Hz), 2.32 (1H, $\nu_{1/2}$ = 80 Hz); the other resonances were not observed.

Cp'_2Ce(4-methylbenzyl). Method A: Cp'_2CeOTf·0.5 hexane[2] (1 g, 1.2 mmol) was dissolved in 50 mL of pentane and 4-methylbenzylmagnesium chloride solution[21] (1.8 mL, 0.69 M in diethyl ether, 1.2 mmol) was added *via* syringe. The solution immediately changed from yellow to red. After 2 min the solvent was removed under reduced pressure, yielding a red-orange powder. The red solid was extracted with 10 mL of pentane, and the yellow solid residue was extracted further with 25 mL toluene to recover Cp'_2CeCl. The volume of the pentane solution was reduced to 7 mL and cooled to –10 °C, giving red needles. Yield, 0.48 g (0.68 mmol, 56%). MP 119–122 °C (sample turned purple on melting). ^1H NMR (C_6D_{12}): δ 40.65 (2H, $\nu_{1/2}$ = 300 Hz), 13.60 (2H, $\nu_{1/2}$ = 250 Hz), 0.27 (3H, 5 Hz), –0.57 (36H, $\nu_{1/2}$ = 40 Hz), –10.91 (18H, $\nu_{1/2}$ = 150 Hz). Anal. Calcd. for $C_{42}H_{67}Ce$: C, 70.8; H, 9.48. Found C, 70.9; H, 9.41.

Method B: $Cp'_2CeCH_2C_6H_5$[2] was dissolved in *p*-xylene in an NMR tube and heated at 60 °C for 2 days. The red solution was taken to dryness and the red solid residue was dissolved in C_6D_{12}. The ^1H NMR spectrum was identical to that of the red crystals obtained *via* Method A.

NMR tube equilibration of Cp'_2Ce(4-methylbenzyl) in C_6D_{12}

Cp'_2Ce(4-methylbenzyl) was dissolved in C_6D_{12} in an NMR tube and allowed to stand. After one day at 19 °C, the red solution had turned purple and resonances due to the metallacycle $Cp'[(Me_3C)_2C_5H_2C(Me)_2CH_2]Ce$[2] and *p*-xylene had appeared in the ^1H NMR spectrum. The ratio of Cp'_2Ce(4-methylbenzyl) and $Cp'[(Me_3C)_2C_5H_2C(Me)_2CH_2]Ce$ was approximately 1 : 1. After two days, the ratio was 1 : 2.5. After 5 days, the ratio was 1 : 4. The ratio did not change upon further standing.

Solid state H-for-D exchange in $Cp'_2CeCD_2C_6D_5$

A crystalline sample of $Cp'_2CeCD_2C_6D_5$ was allowed to stand at 20–25 °C for 1430 days. A small amount of the sample was dissolved in C_6D_6, and the ^1H NMR spectrum was as described above for the fresh sample. The ^2H NMR spectrum contained the aromatic benzyl group resonances at δ 4.18 and 2.32, and also a resonance at δ –13.15 ($\nu_{1/2}$ = 100 Hz) with an integrated intensity equal to roughly two deuterons relative to the benzyl ligand resonances. The sample was hydrolyzed and filtered. The ^1H NMR spectrum of the hydrolysate contained a sharp singlet at 2.120 ppm and a weak 1 : 1 : 1 pattern (J_{HD} = 1.8 Hz) at 2.105 ppm due to $C_6D_5CH_3$ and $C_6D_5CDH_2$, respectively. No resonances due to the aromatic toluene CH-groups were observed. Six Cp′H-CMe_3 resonances were also present in the spectrum, δ 1.38, 1.32, 1.27, 1.19, 1.15, and 1.09 ppm in a 1 : 1 : 2 : 1.5 : 1 : 2 area ratio, arising from two Cp′H isomers.[12] The ^2H NMR spectrum contained a triplet at 2.05 ppm (J_{HD} = 2.1 Hz) due to $C_6D_5CDH_2$ and a single broadened CMe_3-d_x resonance at 1.13 ppm ($\nu_{1/2}$ = 4 Hz). Aromatic toluene ^2H resonances were masked by the solvent peak. Another sample of aged $Cp'_2CeCD_2C_6D_5$ was dissolved in C_6H_{12} and hydrolyzed. The ^2H NMR spectrum contained three aromatic resonances at 7.27, 7.16, and 7.09 ppm, the CDH_2 triplet at 2.29 ppm, and the single broad CMe_3 resonance at 1.12 ppm in a 3 : 9 : 16 : 1 : 16 area ratio.

The sample in C_6D_6 was heated at 60 °C for 2 days. Three Cp′H-CMe_3-resonances were present in the ^1H NMR spectrum, δ 1.26, 1.18, 1.08 ppm in a 9 : 6.5 : 9 area ratio. A broadened peak at 1.16 ppm was also observed, presumably due to CMe_3-d_x groups. The ^{13}C NMR contained three resonances due to the CMe_3 groups, δ 32.58, 30.83, and 30.12 ppm. A 1 : 1 : 1 pattern at 30.10 ppm (J_{CD} = 3.6 Hz) was consistent with the presence of CMe_2CDH_2 groups. GC-MS analysis showed the presence of partially deuterated toluene and partially deuterated Cp′H. Molecular ion isotope pattern for toluene: $(M–1 \text{ or } 2)^+$ m/z (relative abundance): 92 (3), 93 (6), 94 (12), 95 (74), 96 (100), 97 (96), 98 (24), 99 (2). For Cp′H, $(M)^+$ m/z (calculated relative abundance for $C_{17}H_{30}$/found): 234 (100/100), 235 (19/76), 236 (2/61), 237 (0.1/13), 238 (0.004/2), giving the observed ratio of Cp′H, Cp′H-d_1, and Cp′H-d_2 as 35 : 20 : 17.

NMR tube equilibration of $Cp'_2Ce(CH_2C_6H_5)$ isomers in toluene-h_8

$Cp'_2Ce(CH_2Ph)$ was dissolved in toluene-h_8 and heated at 60 °C for 1 day, then allowed to stand at 19 °C for one day, yielding a deep red solution. The ^1H NMR spectrum contained resonances due to $Cp'_2Ce(CH_2Ph)$ and $Cp'[(Me_3C)_2C_5H_2C(Me)_2CH_2]Ce$ in a 12 : 1 area ratio, as well as four new paramagnetic resonances, ^1H NMR (C_7H_8, 400 MHz): δ –1.585 ($\nu_{1/2}$ = 40 Hz), –1.771 ($\nu_{1/2}$ = 40 Hz), –9.716 ($\nu_{1/2}$ = 40 Hz), –10.216 ($\nu_{1/2}$ = 40 Hz), in approximately a 1 : 3 : 1.5 : 1 area ratio. Assuming that the resonances at –9.716 and –10.216 correspond to the unique CMe_3 resonances of two different Cp'_2Ce-R complexes, the ratio of $Cp'_2Ce(CH_2Ph)$, $Cp'[(Me_3C)_2C_5H_2C(Me)_2CH_2]C$ and the two new species was 12 : 1 : 3 : 2. The sample was hydrolyzed with D_2O and filtered. The ^2H NMR spectrum contained two Cp′D ring C–D resonances at 3.115 (d, J_{HD} = 3 Hz) and 2.966 (s) in a 3 : 4 area ratio, and resonances due to toluene-d_1 at 7.174, 7.095, 7.067, and 2.16 (t, J_{HD} = 2.1 Hz) in a 2.5 : 1 : 1 : 6 area ratio.

NMR tube equilibration of $(Cp'\text{-}d_{27})_2Ce(CD_2C_6D_5)$ isomers in toluene-d_8

$Cp'_2Ce(CH_2Ph)$ was dissolved in C_6D_6 and heated at 60 °C for 4 days to perdeuterate the CMe_3 groups. The sample was taken to dryness and the solid residue was dissolved in fresh C_6D_6. The sample was heated for an additional 4 days, then taken to dryness, and the solid residue was dissolved in toluene-d_8. The sample was heated at 60 °C for 1 day, and then allowed to stand at 19 °C for one day. The sample was taken to dryness and the solid residue was dissolved in cyclohexane-d_{12}. The ^2H NMR spectrum contained $C(CD_3)_3$ resonances due to $(Cp'\text{-}d_{27})_2Ce(CD_2C_6D_5)$ and the two new species observed in the previous experiment in a 2 : 1 : 1 area ratio. The sample was hydrolyzed with H_2O and filtered. The ^1H NMR spectrum contained multiple Cp′H ring resonances, as well as resonances due to isomers of toluene-d_7 at 7.108, 7.038, and 2.246. Subtracting the area of the residual toluene peaks in the cyclohexane-d_{12} solution before hydrolysis relative to an internal standard indicated that the resonances had increased in intensity after hydrolysis in an approximate 1 : 1 : 3 area ratio.

NMR tube reaction of CH_3F and $Cp'_2Ce(CH_2C_6H_5)$ in benzene-d_6

$Cp'_2Ce(CH_2C_6H_5)$ was dissolved in C_6D_6 in an NMR tube. The tube was cooled in a liquid nitrogen isopropanol bath, the head space was evacuated, and replaced with CH_3F (1 atm). The tube was warmed to 19 °C and allowed to stand. After 1 day, resonances in the ^1H NMR spectrum due to Cp'_2CeF had appeared; the ratio of $Cp'_2Ce(CH_2C_6H_5)$ to Cp'_2CeF was 2 : 1. Resonances due to Cp″Cp′CeF had also appeared (Cp″ is Cp′+CH_2),[1,4] as well as $CH_3C_6H_5$ and $CH_3CH_2C_6H_5$ in a 4 : 1 area ratio. After 2 days, all $Cp'_2Ce(CH_2C_6H_5)$ resonances had disappeared from the ^1H NMR spectrum. Integration of the CMe_3 signal intensities relative to the residual solvent proton signal indicated that slightly less than half an equivalent of Cp'_2CeF had formed relative to the starting material.

NMR tube reaction of CH_3F and $Cp'_2Ce(CD_2C_6D_5)$ in benzene-d_6

$Cp'_2Ce(CD_2C_6D_5)$ was dissolved in C_6D_6 in an NMR tube. The tube was cooled in a liquid nitrogen isopropanol bath, the head space was evacuated, and replaced with CH_3F (1 atm). The tube was warmed to 19 °C and allowed to stand. After 1 day, resonances in the ^1H NMR spectrum due to Cp'_2CeF had appeared; the ratio of $Cp'_2Ce(CD_2C_6D_5)$ to Cp'_2CeF was 1 : 2. Resonances due to Cp″Cp′CeF had also appeared, along with a singlet at 1.05 ppm and a broad hump at 2.4 ppm presumably corresponding to the CH_3 and residual protons in the CD_2 group of $CH_3CD_2C_6D_5$, respectively. After 2 days, all $Cp'_2Ce(CD_2C_6D_5)$ resonances had disappeared from the ^1H NMR spectrum. Integration of the CMe_3 signal intensities relative to the residual solvent proton signal indicated that slightly less than half an equivalent of Cp'_2CeF had formed relative to the starting material. The ^2H NMR spectrum contained resonances due to C_6D_6, $CHD_2C_6D_5$, and a multiplet at 2.35 ppm presumably corresponding to the CD_2 group of $CH_3CD_2C_6D_5$. No signal was observed at 1.05 ppm in the ^2H NMR spectrum. GC-MS analysis showed three principle components in addition to Cp′H, with $(M-2)^+$ m/z 97 ($CHD_2C_6D_5$), 113 ($CH_3CD_2C_6D_5$), and $(M)^+$ 248 (Cp″H) in an approximate ratio of 1 : 1 : 6.

NMR tube reaction of CH_3F and $Cp'_2Ce(C_6H_5)$ in benzene-h_6

$Cp'_2Ce(CH_2C_6H_5)$ was dissolved in cyclohexane-d_{12} and heated at 60 °C for 12 h, yielding a solution of $Cp'[(Me_3C)_2C_5H_2C(Me)_2CH_2]Ce$. The sample was taken to dryness, dissolved in cyclohexane-d_{12}, and heated at 60 °C for 12 h to remove residual toluene. The sample was taken to dryness, dissolved in benzene-h_6, and heated at 60 °C for 12 h, yielding a very deep red solution of $Cp'_2Ce(C_6H_5)$.[2] The tube was cooled in a liquid nitrogen isopropanol bath, the head space was evacuated, and replaced with CH_3F (1 atm). The tube was warmed to 19 °C and allowed to stand. After 1 h, resonances in the ^1H NMR spectrum due to Cp'_2CeF and Cp″Cp′CeF had appeared; the ratio of $Cp'_2Ce(C_6H_5)$ to the two fluoride species was 30 : 1. After 2 days, the ratio was 6 : 5, and a diamagnetic singlet had appeared at 2.10 ppm, suggesting the formation of toluene. After 5 days, the ratio was 1 : 4. GC-MS analysis indicated the presence of toluene. Cp′H and Cp″H were the only other major components besides C_6H_6.

NMR tube reaction of CH_3F and $(Cp'\text{-}d_{27})_2Ce(C_6D_5)$ in benzene-d_6

$Cp'_2Ce(CH_2C_6H_5)$ was dissolved in benzene-d_6 and heated at 60 °C for 2 days. The sample was taken to dryness, dissolved in fresh benzene-d_6, and heated at 60 °C for 2 days. This procedure was repeated two more times, with the sample heated for 8 days after the last addition of benzene-d_6, yielding a solution of $(Cp'\text{-}d_{27})_2Ce(C_6D_5)$. The sample was taken to dryness, and dissolved in fresh benzene-d_6. The tube was cooled in a liquid nitrogen isopropanol bath, the head space was evacuated, and replaced with CH_3F (1 atm). The tube was warmed to 19 °C and allowed to stand. After 3 days, resonances in the ^2H NMR spectrum matching those observed in the ^1H NMR spectrum of the previous experiment, presumably due to $(Cp'\text{-}d_{27})_2CeF$ and $(Cp''\text{-}d_{27})(Cp'\text{-}d_{27})CeF$ had appeared; the ratio of $(Cp'\text{-}d_{27})_2Ce(C_6D_5)$ to the two fluoride species was 4 : 1. A diamagnetic singlet had appeared at 2.10 ppm in the ^1H NMR, suggesting the formation of toluene. After 2 additional days, the ratio was 6 : 5. After 11 days, the ratio of $(Cp'\text{-}d_{27})_2Ce(C_6D_5)$ to the two fluoride species was 1 : 1. After 42 days, only the two fluoride species remained in the ^2H NMR. GC-MS analysis indicated the presence of toluene-d_5, $(M-1)^+$ m/z 96. $(Cp'\text{-}d_{27})H$ and $(Cp''\text{-}d_{27})H$ were the only other major components besides C_6D_6.

NMR tube reaction of CH_3Cl, CH_3Br, and CH_3I with $Cp'_2Ce(CH_2C_6H_5)$ in cyclohexane-d_{12}

$Cp'_2Ce(CH_2C_6H_5)$ was dissolved in cyclohexane-d_{12} in an NMR tube. The tube was cooled in a liquid nitrogen isopropanol bath, and the head space was evacuated. In the case of CH_3Cl and CH_3Br, the head space was filled with the halomethane gas (1 atm). In the case of CH_3I, an excess was added by vacuum transfer and the head space was backfilled with N_2. The sample was warmed to 19 °C and allowed to stand. In the case of CH_3Cl, after 10 min, resonances of the same intermediate complex observed in the reaction of CH_3Cl with $Cp'[(Me_3C)_2C_5H_2C(Me)_2CH_2]Ce$, Cp'_2CeCH_2Cl[4] had appeared in the ^1H NMR spectrum; the ratio of $Cp'_2Ce(CH_2C_6H_5)$ and Cp'_2CeCH_2Cl was approximately 32 : 1. After three days, only resonances due to Cp'_2CeCl remained in the ^1H NMR spectrum, and yellow crystals of Cp'_2CeCl had formed. Diamagnetic resonances due to $CH_3C_6H_5$ and $CH_3CH_2C_6H_5$ had also appeared. In the case of CH_3Br, after 19 h, resonances due Cp'_2CeBr and Cp'_2CeCH_2Br[4] had appeared in the ^1H NMR spectrum; the ratio of $Cp'_2Ce(CH_2C_6H_5)$, Cp'_2CeBr, and Cp'_2CeCH_2Br was approximately 1.5 : 7 : 1. Diamagnetic resonances due to $CH_3C_6H_5$ and $CH_3CH_2C_6H_5$ had also appeared. After five days, only resonances due to Cp'_2CeBr remained in the ^1H NMR spectrum, and orange crystals of Cp'_2CeBr had formed. In the case of CH_3I, after three hours, resonances due Cp'_2CeI and Cp'_2CeCH_2I[4] had appeared in the ^1H NMR spectrum; the ratio of $Cp'_2Ce(CH_2C_6H_5)$, Cp'_2CeI, and Cp'_2CeCH_2I was approximately 75 : 10 : 1. After 24 h, resonances due to $Cp'_2Ce(CH_2C_6H_5)$ had disappeared from the ^1H NMR spectrum. Paramagnetic resonances due to Cp'_2CeI and Cp'_2CeCH_2I were present in a 3 : 1 ratio, and diamagnetic resonances due to $CH_3C_6H_5$ and $CH_3CH_2C_6H_5$ had also appeared. After five days, the ratio was 24 : 1. After 11 days, orange crystals had formed, and only resonances due to Cp'_2CeI remained in the spectrum. The GC-MS analysis of all three samples showed three principle components in addition to

Cp′H, with $(M-1)^+$ *m*/*z* 91 ($CH_3C_6H_5$), 106 ($CH_2C_6H_5$+CH_3), and $(M)^+$ 248 (Cp″H).

NMR tube reaction of CD_3Br or CD_3I and $Cp'_2Ce(CH_2C_6H_5)$ in benzene-d_6

$Cp'_2Ce(CH_2C_6H_5)$ was dissolved in benzene-d_6 in an NMR tube. The tube was cooled in a liquid nitrogen isopropanol bath, and the head space was evacuated. In the case of CD_3Br, the head space was filled with the gas (1 atm); in the case of CD_3I, an excess was added by vacuum transfer, and the head space was backfilled with N_2. The tube was warmed to 19 °C and allowed to stand. In the case of CD_3Br, after 24 h, resonances due to $Cp'_2Ce(CH_2C_6H_5)$ had disappeared from the ^{1}H NMR spectrum and resonances due to Cp'_2CeBr had appeared. In the case of CD_3I, after 24 h, resonances due to Cp'_2CeI had appeared in the ^{1}H NMR spectrum, and the ratio of $Cp'_2Ce(CH_2C_6H_5)$ to Cp'_2CeI was 1 : 18. After 2 days, resonances due to $Cp'_2Ce(CH_2C_6H_5)$ had disappeared from the ^{1}H NMR spectrum. In both cases, a broad multiplet at 1.05 ppm presumably corresponding to residual protons in the CD_3 group and a singlet at 2.4 ppm presumably corresponding to the CH_2 group of $CD_3CH_2C_6H_5$ had also appeared in a 1 : 2 ratio. Integration of the CMe_3 signal intensities relative to the residual solvent proton signal indicated approximately 70% conversion of $Cp'_2Ce(CH_2C_6H_5)$ to Cp'_2CeBr and 85% conversion of $Cp'_2Ce(CH_2C_6H_5)$ to Cp'_2CeI. The ^{2}H NMR spectra in both cases contained resonances due to C_6D_6, CD_3Br or CD_3I, and a multiplet at 0.98 ppm presumably corresponding to the CD_3 group of $CD_3CH_2C_6H_5$. No signal was observed at 2.4 ppm due to deuteria in the benzylic sites in either ^{2}H NMR spectrum. GC-MS analysis showed three principle components in addition to Cp′H, with $(M-1)^+$ *m*/*z* 91 ($CH_3C_6H_5$), 108 ($CH_2C_6H_5$+CD_3), and $(M)^+$ 251 (Cp′H+CD_2).

NMR tube reaction of CD_3Br and $Cp'_2Ce(CH_2C_6H_5)$ in benzene-h_6

$Cp'_2Ce(CH_2C_6H_5)$ was dissolved in C_6H_6 in an NMR tube. The tube was cooled in a liquid nitrogen isopropanol bath, the head space was evacuated, and replaced with CD_3Br (1 atm). The tube was warmed to 19 °C and allowed to stand. After 24 h, the sample was cooled in a liquid nitrogen isopropanol bath maintained at –20 °C, the head space was evacuated, the tube cap was closed, and the sample was warmed to 19 °C. This freeze–pump–thaw procedure was performed two more times to remove residual CD_3Br. A yellow precipitate formed, and the yellow solution was filtered into a clean tube. The ^{2}H NMR spectrum of the solution contained resonances due to CD_3Br and a singlet at 1.06 ppm presumably corresponding to the CD_3 group of $CD_3CH_2C_6H_5$. No signal was observed at 2.4 ppm in the ^{2}H NMR spectrum.

NMR tube reaction of CH_3F and Cp'_2Ce(4-methylbenzyl) in C_6D_{12}

Cp'_2Ce(4-methylbenzyl) was dissolved in C_6D_{12} in an NMR tube. The tube was cooled in a liquid nitrogen isopropanol bath, the head space was evacuated, and replaced with CH_3F (1 atm). The tube was warmed to 19 °C and allowed to stand. After 1 day, resonances in the ^{1}H NMR spectrum due to Cp'_2CeF had appeared; the ratio of Cp'_2Ce(4-methylbenzyl) to Cp'_2CeF was 1 : 1. Resonances due to Cp″Cp′CeF and *p*-xylene had also appeared, along with new diamagnetic resonances at 6.96 (4H, s), 2.52 (2H, q), 2.24 (3H, s), and 1.17 (3H, t), apparently due to 4-ethyltoluene. After 2 days, all Cp'_2Ce(4-methylbenzyl) resonances had disappeared from the ^{1}H NMR spectrum. Integration of the CMe_3 signal intensities relative to the residual solvent proton signal indicated that approximately 70% of the starting material had been converted to Cp'_2CeF. The GC-MS analysis showed three principle components in addition to Cp′H, with $(M-1)^+$ *m*/*z* 106 ($CH_3C_6H_4CH_3$), 120 ($CH_3CH_2C_6H_4CH_3$), and $(M)^+$ 248 (Cp″H).

NMR tube reaction of CH_3Cl, CH_3Br, or CH_3I and Cp'_2Ce(4-methylbenzyl) in C_6D_{12}

Cp'_2Ce(4-methylbenzyl) was dissolved in C_6D_{12} in an NMR tube. The tube was cooled in a liquid nitrogen isopropanol bath, and the head space was evacuated. In the case of CH_3Cl and CH_3Br, the head space was refilled with the halomethane gas (1 atm). In the case of CH_3I, an excess was added by vacuum transfer, and the head space was backfilled with N_2. In the case of CH_3Cl, after 3 days, all Cp'_2Ce(4-methylbenzyl) resonances had disappeared from the ^{1}H NMR spectrum, and orange crystals of Cp'_2CeCl had formed. In the case of CH_3Br, after 30 min, resonances due to Cp'_2CeCH_2Br and Cp'_2CeBr had appeared in the ^{1}H NMR spectrum; the ratio of Cp'_2Ce(4-methylbenzyl) to Cp'_2CeCH_2Br and Cp'_2CeBr was 20 : 1 : 1. After 17 h, the ratio was 2.5 : 1 : 75. After 2 days, all Cp'_2Ce(4-methylbenzyl) and Cp'_2CeCH_2Br resonances had disappeared from the ^{1}H NMR spectrum, and orange crystals of Cp'_2CeBr had formed. In the case of CH_3I, after 30 min, resonances due to Cp'_2CeCH_2I had appeared in the ^{1}H NMR spectrum; the ratio of Cp'_2Ce(4-methylbenzyl) to Cp'_2CeCH_2I was 21 : 1. After 2 days, all Cp'_2Ce(4-methylbenzyl) resonances had disappeared from the ^{1}H NMR spectrum and resonances due to Cp'_2CeI had appeared. The ratio of Cp'_2CeCH_2I to Cp'_2CeI was 1 : 6. In all cases, diamagnetic resonances due to *p*-xylene and 4-ethyltoluene also appeared in the ^{1}H NMR spectrum, and GC-MS analysis showed four principle components in addition to Cp′H, with $(M-1)^+$ *m*/*z* 106 ($CH_3C_6H_4CH_3$), 120 ($CH_3CH_2C_6H_4CH_3$), and $(M)^+$ 248 (Cp″H).

NMR tube reaction of CD_3Br and Cp'_2Ce(4-methylbenzyl) in C_6H_{12}

Cp'_2Ce(4-methylbenzyl) was dissolved in C_6H_{12} in an NMR tube. The tube was cooled in a liquid nitrogen isopropanol bath, the head space was evacuated, the sample was warmed to 19 °C, and the head space was refilled with CD_3Br (1 atm). After 20 min, resonances due to Cp'_2CeCD_2Br and Cp'_2CeBr had appeared in the ^{1}H NMR spectrum; the ratio of Cp'_2Ce(4-methylbenzyl) to Cp'_2CeCD_2Br and Cp'_2CeBr was 100 : 1 : 4. After 2 days, all Cp'_2Ce(4-methylbenzyl) and Cp'_2CeCD_2Br resonances had disappeared from the ^{1}H NMR spectrum, and orange crystals of Cp'_2CeBr had formed. Diamagnetic resonances at 6.92 and 6.95 ppm corresponding to the aromatic protons of *p*-xylene and 4-ethyltoluene had also appeared. A diamagnetic resonance had appeared in the ^{2}H NMR spectrum at δ 1.17 corresponding to the -CH_2CD_3 group of 4-ethyltoluene; the intense resonance due to excess CD_3Br masked the region where a resonance due to deuterium bound to the secondary carbon of the ethyl group would have been observed. The GC-MS analysis showed four principle components in addition to Cp′H, with $(M-1)^+$ *m*/*z* 106

($CH_3C_6H_4CH_3$), 122 ($CH_3C_6H_4CH_3$+CD_2), and $(M)^+$ m/z 251 (Cp′H+CD_2).

NMR tube reaction of CD_3I and Cp'_2Ce(4-methylbenzyl) in C_6D_6

Cp'_2Ce(4-methylbenzyl) was dissolved in C_6D_6 in an NMR tube. The tube was cooled in a liquid nitrogen isopropanol bath, the head space was evacuated, the sample was warmed to 19 °C, an excess of CD_3I was added by vacuum transfer, and the head space was backfilled with N_2. After 1 day, all Cp'_2Ce(4-methylbenzyl) resonances had disappeared and resonances due to Cp'_2CeCD_2I and Cp'_2CeI had appeared in the ^1H NMR spectrum from the ^1H NMR spectrum. Diamagnetic resonances at 6.92 and 6.95 ppm corresponding to the aromatic protons of *p*-xylene and 4-ethyltoluene had also appeared. A diamagnetic resonance had appeared in the ^2H NMR spectrum at δ 1.02 corresponding to the -CH_2CD_3 group of 4-ethyltoluene. No resonance was observed at 2.55 ppm which would have indicated deuteration at the secondary position in the ethyl group. The GC-MS analysis showed four principle components in addition to Cp′H, with $(M-1)^+$ m/z 106 ($CH_3C_6H_4CH_3$), 122 ($CH_3C_6H_4CH_3$+CD_2), and $(M)^+$ m/z 251 (Cp′H+CD_2).

Crystallographic studies of $Cp'_2Ce(CH_2C_6H_5)$ and Cp'_2Ce(4-methylbenzyl)

Single crystals of appropriate dimension were mounted on glass fibers or Kapton loops using Paratone N hydrocarbon oil. All measurements were made on a SMART 1000[22] diffractometer with a CCD area detector and graphite monochromated Mo-Kα radiation. Data were collected at low temperature using 10 s ω or ω and ϕ scans. Frame data were integrated using SAINT[23] and empirical absorption corrections were applied using SADABS.[24] The data were also corrected for Lorentz-polarisation effects. The structures were solved using direct methods[25] and expanded using Fourier techniques.[26] Non-hydrogen atoms were refined anisotropically. Hydrogen atoms were included in calculated positions but not refined. All calculations for $Cp'_2Ce(CH_2C_6H_5)$ were performed using the teXsan[27] crystallographic software package of Molecular Structure Corporation. All calculations for Cp'_2Ce(4-methylbenzyl) were performed using the SHELXTL[28] crystallographic software package of Bruker Analytical X-ray Systems Inc. Crystallographic data are given in Table 1 and full crystallographic details are included in the ESI.†

Table 1 Crystallographic data

Compound	$Cp'_2CeCH_2C_6H_5$	Cp'_2Ce(4-methylbenzyl)·0.5(pentane)
Empirical Formula	$C_{41}H_{65}Ce$	$C_{44.25}H_{72.5}Ce$
Formula Weight	698.05	744.64
T/K	179(2)	120(2)
Crystal System	Triclinic	Triclinic
Space Group	$P\bar{1}$	$P\bar{1}$
a/Å	13.228(1)	10.528(2)
b/Å	16.080(1)	12.032(3)
c/Å	18.499(1)	17.562(4)
α (°)	96.377(1)	84.069(4)
β (°)	105.388(1)	79.816(4)
γ (°)	96.173(1)	66.418(3)
V/Å^3	3731.57(14)	2005.4(8)
Z	4	2
Unique Reflections (R_{int})	12450 (0.0229)	7273 (0.0821)
R_1, wR_2[a]	0.0361, 0.0707	0.0493, 0.0933

[a] R_1 based on selected data with $I > 2\sigma(I)$; wR_2 based on all data.

Computational details

The Stuttgart–Dresden–Bonn Relativistic large Effective Core Potential (RECP)[29a] has been used to represent the inner shells of Ce. The associated basis set of the type (7s6p5d)/[5s4p3d] augmented by an f polarization function ($\alpha = 1.000$)[29b] has been used to represent the valence orbitals. F has also been represented by an RECP with the associated basis set of the type (4s5p/2s3p) augmented by two contracted *d* polarisation Gaussian functions ($\alpha_1 = 3.3505(0.357851)$, $\alpha_2 = 0.9924(0.795561)$).[30] C and H have been represented by an all-electron 6-31G(d,p) basis set.[31] Calculations have been carried out at the DFT(B3PW91)[32] level with Gaussian 98.[33] The nature of the extrema (minimum or transition state) has been established with analytical frequency calculations and the intrinsic reaction coordinate (IRC) has been followed to confirm that transition states connect to reactants and products. The zero point energy (ZPE) and entropic contribution have been estimated within the harmonic potential approximation. The Gibbs free energy, G, was calculated for $T = 298.15$ K and 1 atm. The NBO analysis[34] was carried out replacing Ce by La because of the technical requirement to have an even number of f electrons for the calculations. This method has been used successfully in previous studies.[1,2,34b]

Acknowledgements

This work was supported by the Director, Office of Science, Office of Basic Energy Sciences (OBES), of the U.S. Department of Energy (DOE) under Contract No. DE-AC02-05CH11231. We thank F. J. Hollander and A. G. DiPasquale at CHEXRAY, the U.C. Berkeley X-ray diffraction facility, for help with the crystallography. L.M thanks the CINES and CALMIP for a generous grant of computing time. L.M. is also a junior member of the Institut Universitaire de France, L.M. and O.E thank the CNRS and Ministère de l'Enseignement Supérieur et de la Recherche for funding.

References

1 E. L. Werkema, E. Messines, L. Perrin, L. Maron, O. Eisenstein and R. A. Andersen, *J. Am. Chem. Soc.*, 2005, **127**, 7781.
2 L. Maron, E. Werkema, L. Perrin, O. Eisenstein and R. A. Andersen, *J. Am. Chem. Soc.*, 2005, **127**, 279.
3 E. L. Werkema and R. A. Andersen, *J. Am. Chem. Soc.*, 2008, **130**, 7153.
4 E. L. Werkema, R. A. Andersen, A. Yahia, L. Maron and O. Eisenstein, *Organometallics*, 2009, **28**, 3173.
5 M. Booij, A. Meetsma and J. H. Teuben, *Organometallics*, 1991, **10**, 3246.
6 G. R. Davies, J. A. J. Jarvis and B. T. Kilbourn, *J. Chem. Soc. D*, 1971, 1511.
7 I. W. Bassi, G. Allegra, R. Scordamaglia and G. Chioccola, *J. Am. Chem. Soc.*, 1971, **93**, 3787.
8 G. R. Davies, J. A. J. Jarvis, B. T. Kilbourn and A. J. P. Pioli, *J. Chem. Soc. D*, 1971, 677.
9 P. G. Edwards, R. A. Andersen and A. Zalkin, *Organometallics*, 1984, **3**, 293.
10 E. A. Mintz, K. G. Moloy, T. J. Marks and V. W. Day, *J. Am. Chem. Soc.*, 1982, **104**, 4692.

11 J. L. Kiplinger, D. E. Morris, B. L. Scott and C. J. Burns, *Organometallics*, 2002, **21**, 5978.
12 G. Zi, L. Jia, E. L. Werkema, M. D. Walter, J. P. Gottfriedsen and R. A. Andersen, *Organometallics*, 2005, **24**, 4251.
13 L. Maron, L. Perrin and O. Eisenstein, *J. Chem. Soc., Dalton Trans.*, 2002, 534.
14 C. H. Langford, and H. B. Gray, *"Ligand Substitution Processes"* W. A. Benjamin, Inc. New York, NY, 1966.
15 S. G. Lias, J. E. Bartmess, J. F. Liebman, J. L. Holmes, R. D. Levin and W. G. Mallard, *J. Phys. Chem. Ref. Data*, 1988, **17**, 647.
16 C. Pellecchia, A. Immirzi, D. Pappalardo and A. Peluso, *Organometallics*, 1994, **13**, 3773.
17 C. A. Cruz, D. J. H. Emslie, L. E. Harrington and J. F. Britten, *Organometallics*, 2008, **27**, 15.
18 C. A. Cruz, D. J. Emslie, C. M. Robertson, L. E. Harrington, H. A. Jenkins and J. F. Britten, *Organometallics*, 2009, **28**, 1891.
19 D. Hoffmann, W. Bauer, F. Hampel, N. J. R. van Eikema Hommes, P. v. R. Schleyer, P. Otto, U. Pieper, D. Stalke, D. S. Wright and R. Snaith, *J. Am. Chem. Soc.*, 1994, **116**, 528.
20 E. L. Werkema, L. Maron, O. Eisenstein and R. A. Andersen, *J. Am. Chem. Soc.*, 2007, **129**, 2529.
21 J. S. Hallock, A. S. Galiano-Roth and D. B. Collum, *Organometallics*, 1988, **7**, 2486.
22 *SMART: Area-Detector Software Package*, Bruker Analytical X-ray Systems, Inc.: Madison, WI, 1995-99.
23 *SAINT: SAX Area-Dectector Integration Program, V7.06*Siemens Industrial Automation, Inc.: Madison, WI, 2005.
24 *SADABS: (v2.10) Siemens Area Detector ABSorption correction program*, George Sheldrick, 2005 .
25 For $Cp'_2Ce(CH_2C_6H_5)$, SIR92:A. Altomare, M. C. Burla, M. Camalli, M. Cascarano, C. Giacovazzo, A. Guagliardi and G. Polidori, *J. Appl. Crystallogr.*, 1993, **26**, 343; For Cp'_2Ce(4-methylbenzyl), XS:; *Program for the Solution of X-ray Crystal Structures, Part of the SHELXTL Crystal Structure Determination Package*, Bruker Analytical X-ray Systems Inc.: Madison, WI, 1995-99.
26 For $Cp'_2Ce(CH_2C_6H_5)$, DIRDIF92: P. T. Beurskens, G. Admiraal, G. Beurskens, W. P. Bosman, S. Garcia-Granda, R. O. Gould, J. M. M. Smits, and C. Smykalla, 1992.*The DIRDIF program system, Technical Report of the Crystallography Laboratory*, University of Nijmegen, The Netherlands; For Cp'_2Ce(4-methylbenzyl), XL:; *Program for the Refinement of X-ray Crystal Structures, Part of the SHELXTL Crystal Structure Determination Package*, Bruker Analytical X-ray Systems Inc.: Madison, WI, 1995-99.
27 teXsan: *Crystal Structure Analysis Package*, Molecular Structure Corporation (1985 & 1992).
28 XP: *Molecular Graphics program. Part of the SHELXTL Structure Determination Package*. Bruker Analytical X-ray Systems Inc.: Madison, WI, (1995-99).
29 (*a*) M. Dolg, H. Stoll, A. Savin and H. Preuss, *Theor. Chim. Acta*, 1989, **75**, 173; M. Dolg, H. Stoll and H. Preuss, *Theor. Chim. Acta*, 1993, **85**, 441; (*b*) L. Maron and O. Eisenstein, *J. Phys. Chem. A*, 2000, **104**, 7140.
30 L. Maron and C. Teichteil, *Chem. Phys.*, 1998, **237**, 105.
31 P. C. Hariharan and J. A. Pople, *Theor. Chim. Acta*, 1973, **28**, 213.
32 (*a*) J. P. Perdew and Y. Wang, *Phys. Rev. B*, 1992, **45**, 13244; (*b*) A. D. Becke, *J. Chem. Phys.*, 1993, **98**, 5648; (*c*) K. Burke, J. P. Perdew, and Y. Wang, in *"Electronic Density Functional Theory: Recent Progress and New Directions"*, J. F. Dobson, G. Vignale, and M. P. Das, Eds, 1998, Plenum.
33 *Gaussian 98 (Revision A.09)*, M. J. Frisch, G. W. Trucks, H. B. Schlegel, G. E. Scuseria, M. A. Robb, J. R. Cheeseman, V. G. Zakrzewski, J. A. Montgomery, Jr., R. E. Stratmann, J. C. Burant, S. Dapprich, J. M. Millam, A. D. Daniels, K. N. Kudin, M. C. Strain, O. Farkas, J. Tomasi, V. Barone, M. Cossi, R. Cammi, B. Mennucci, C. Pomelli, C. Adamo, S. Clifford, J. Ochterski, G. A. Petersson, P. Y. Ayala, Q. Cui, K. Morokuma, D. K. Malick, A. D. Rabuck, K. Raghavachari, J. B. Foresman, J. Cioslowski, J. V. Ortiz, A. G. Baboul, B. B. Stefanov, G. Liu, A. Liashenko, P. Piskorz, I. Komaromi, R. Gomperts, R. L. Martin, D. J. Fox, T. Keith, M. A. Al-Laham, C. Y. Peng, A. Nanayakkara, C. Gonzalez, M. Challacombe, P. M. W. Gill, B. G. Johnson, W. Chen, M. W. Wong, J. L. Andres, M. Head-Gordon, E. S. Replogle, and J. A. Pople, Gaussian, Inc., Pittsburgh PA, 1998.
34 (*a*) A. E. Reed, L. A. Curtiss and F. Weinhold, *Chem. Rev.*, 1988, **88**, 899; (*b*) L. Perrin, L. Maron and O. Eisenstein, *Faraday Discuss.*, 2003, **124**, 25; E. D. Brady, D. L. Clark, J. C. Gordon, P. J. Hay, D. W. Keogh, R. Poli, B. L. Scott and J. G. Watkin, *Inorg. Chem.*, 2003, **42**, 6682.

